Wild-type and Brachyolmia-causing Mutant TRPV4 Channels Respond Directly to Stretch Force*[s]

Stephen Loukin[‡1], Xinliang Zhou[‡], Zhenwei Su[‡], Yoshiro Saimi[‡], and Ching Kung[‡§]

From the ‡Laboratory of Molecular Biology and §Department of Genetics, University of Wisconsin, Madison, Wisconsin 53706

Whether animal ion channels functioning as mechanosensors are directly activated by stretch force or indirectly by ligands produced by the stretch is a crucial question. TRPV4, a key molecular model, can be activated by hypotonicity, but the mechanism of activation is unclear. One model has this channel being activated by a downstream product of phospholipase A₂, relegating mechanosensitivity to the enzymes or their regulators. We expressed rat TRPV4 in *Xenopus* oocytes and repeatedly examined >200 excised patches bathed in a simple buffer. We found that TRPV4 can be activated by tens of mm Hg pipette suctions with open probability rising with suction even in the presence of relevant enzyme inhibitors. Mechanosensitivity of TRPV4 provides the simplest explanation of its various force-related physiological roles, one of which is in the sensing of weight load during bone development. Gain-of-function mutants cause heritable skeletal dysplasias in human. We therefore examined the brachyolmia-causing R616Q gain-of-function channel and found increased whole-cell current densities compared with wild-type channels. Single-channel analysis revealed that R616Q channels maintain mechanosensitivity but have greater constitutive activity and no change in unitary conductance or rectification.

In stark contrast with vision, smell, and most tastes, which are based on G-protein-coupled receptors, the mechanical senses (hearing, touch, balance, monitoring blood pressure or systemic osmolarity etc.) are poorly understood in molecular terms. Although prokaryotic mechanosensitive channels are clearly activated directly by membrane stretch force (6), how eukaryotic mechanosensitive channels are activated is still under debate. Models range from direct activation by stretches from membrane and/or cytoskeleton to indirect activation through stretch-produced ligands (7, 8). The mammalian two-pore K⁺ channels TREK1 and TAASK are activated by both membrane stretch and polyunsaturated fatty acids (PUFAs)[2] (9). There, cytoskeletal disruption actually increases mechano-

sensitivity, suggesting that the cytoskeleton does not transmit stretch force to these channels (10).

Among the Ca²⁺-permeable transient receptor potential channels, yeast TRPY1 (11) and animal TRPV4 (transient receptor potential channel subtype V4) (12) have been studied extensively for their response to osmotic or mechanical stimuli. TRPY1 can be activated directly by suctions applied to excised membrane patches (11, 13). However, results from such a test from limited preliminary studies found in the TRPV4 literature are inconsistent and even contradictory (1, 2, 14), likely reflecting mechanical complexities of patches excised from animal cells and/or molecular heterogeneity.

Rodent TRPV4 channels were first cloned repeatedly by following hypotonicity-induced Ca²⁺ signals (1, 2). Rat *trpv4* complements the mechano- and osmosensitivity defects of the *osm-9* mutant worm (15). How osmotic force activates TRPV4 is unclear, however. Besides hypotonicity, this polymodal channel is also activated by PUFAs (16) among other stimuli (12). One study used enzyme inhibitors to block the hypotonicity response and concluded that swelling activates TRPV4 through a specific PUFA, namely 5′,6′-epoxyeicosatrienoic acid, produced by an enzyme pathway comprising phospholipase A₂ (PLA₂) and cytochrome P450 epoxygenase (EPG) (3, 16). This model therefore has the PUFA-producing enzyme(s) or their upstream regulator(s) as the force sensor and TRPV4, a ligand-gated and not a mechanically gated channel. Rat TRPV4 expressed in budding yeast can also be activated by hypotonicity. This finding questions this model because yeast has no PLA₂ or PUFAs (17). Because stretching TRPV4-expressing patches should provide a direct test and because TRPV4 expresses strongly in *Xenopus* oocyte (18), we have undertaken a systematic examination of the possible direct mechanosensitivity of TRPV4 so expressed. Here, we report that TRPV4 is in fact directly mechanosensitive.

Among its many functions, TRPV4 appears to gauge forces sustained by bones. Unloading-induced bone loss is suppressed in *trpv4⁻/⁻* mice (19). Recently, TRPV4 gain-of-function (GOF) mutations were found to cause autosomal dominant blockage of bone development in human. In heterozygotes, clinical manifestations range from post-natal brachyolmia (4), spondylometaphyseal dysplasias, and metatropic dysplasia (5, 20) to infantile and neonatal lethality (5). Expressed in HEK cells, some, although not all, of these GOF alleles present larger whole-cell currents than the wild type (4, 20). No patch-clamp examination of these mutant channels has been reported to date. We conducted an extensive analysis of the brachyolmia-causing R616Q allele and found it to have an increased constitutive activity but also to display direct force activation.

[s] The on-line version of this article (available at http://www.jbc.org) contains supplemental Fig. S1.

[1] To whom correspondence should be addressed: Lab. of Molecular Biology, University of Wisconsin, 1525 Linden Dr., Madison, WI 53706. Tel.: 608-262-7976; Fax: 608-262-4570; E-mail: shloukin@wisc.edu.

[2] The abbreviations used are: PUFA, polyunsaturated fatty acid; PLA₂, phospholipase A₂; EPG, cytochrome P450 epoxygenase; GOF, gain-of-function; 4α-PDD, 4α-phorbol 12,13-didecanoate; BPB, bromophenacyl bromide.
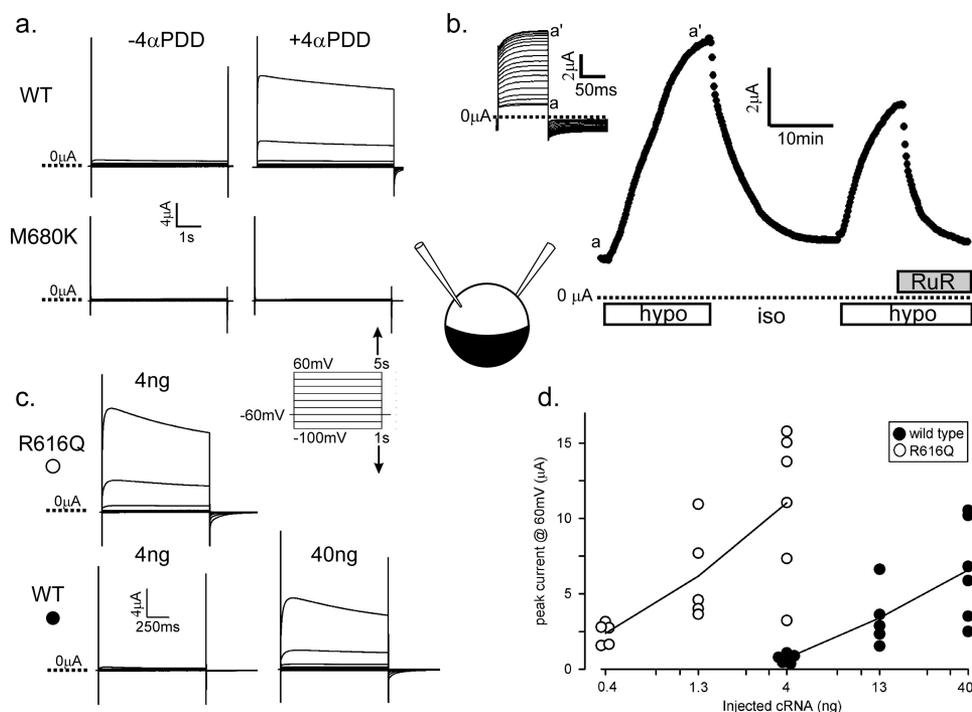
FIGURE 1. **Macroscopic currents of rat TRPV4 expressed in oocytes.** *a*, currents from oocytes expressing wild-type TRPV4 3 days after injection of 4 ng of cDNA (*upper*) and 40 ng of non-conducting M680K TRPV4 (*lower*) upon voltage steps (from −60 mV hold to −100 to +60 mV test in 20-mV increments) before (*left*) and 20 min after (*right*) exposure to 3 μM 4α-PDD. *b*, peak currents from an oocyte expressing very high levels of wild-type TRPV4 (5 days after injection of 40 ng) upon 100-ms voltage steps (from −20 to +20 mV every 10 s) in response to removal of 100 mM sorbitol from the 250 mosM bath solution (*open bars*) and the addition of 3 μM ruthenium red (*RuR; filled bar*). The *inset* shows the raw traces from which peak currents were assessed. (Only every fifth trace from time *a* to *a'* is displayed for clarity.) *hypo*, hypotonic; *iso*, isotonic. *c*, typical currents from oocytes injected with 4 ng of R616Q cRNA (*upper*) or 4 or 40 ng of wild-type cRNA (*lower*). Injections of R616Q RNA above 4 ng killed the oocytes. Tests were performed 3 days after injection with the voltage steps as in *a* but with shorter durations. *d*, expressed currents (assessed at +60 mV) of 15 wild type-expressing oocytes (●) and 15 R616Q-expressing oocytes (○) injected with different amounts of cRNA examined 66–72 h after injection.

EXPERIMENTAL PROCEDURES

Oocyte Expression—Wild-type or mutant alleles were PCR-amplified using high-fidelity *PfuUltra* polymerase (Stratagene) and integrated into pGH19, an oocyte-specific cRNA expression plasmid (21). cRNA was synthesized from XhoI-linearized templates using an mMESSAGE mMACHINE T7 kit (Ambion). Stage V and VI *Xenopus laevis* oocytes were injected with 40 nl of diluted RNA solution. Because TRPV4 expression, particularly of GOF alleles, is toxic to oocytes, 1 μM ruthenium red (Sigma) was added to the ND96 incubation buffer (22). Channel activities increased over several days. Currents were measured after 1–5 days depending on the experimental requirement.

Electrophysiological Techniques—Two-electrode voltage-clamp recording was carried out with HS2A head stages and a VG-2Ax100 virtual bath clamp connected to a GeneClamp 500 amplifier interfaced through a Digidata 1440A digitizer acquired using pClamp10 software (all from Axon Instruments). The base bath solution contained 66 mM KCl, 100 mM sorbitol, 1.8 mM BaCl₂, and 5 mM K⁺-HEPES, pH 7.2 (all from Sigma). 4α-Phorbol 12,13-didecanoate (4α-PDD; 3 μM; Sigma) was added directly to the bath. Sorbitol was omitted from the base solution to form the hypotonic solution. Data were analyzed using both pClamp10 and SigmaPlot 2000 (SPSS) software. Patch clamp was performed with a borosilicate glass

pipette with an ∼1-μm diameter opening at the tip, recorded in excised inside-out mode with symmetric 98 mM KCl, 1 mM MgCl₂, and 10 mM K⁺-HEPES, pH 7.2 (all from Sigma), unless stated otherwise. Data were acquired at 10 kHz through an eight-pole Bessel filter at 1 kHz, played back at >5 kHz for analysis. Suctions were applied through a syringe and gauged with a PX140 pressure sensor (Omega).

RESULTS

Wild-type and R616Q Macroscopic Currents—We examined whole-oocyte currents under two-electrode voltage clamp. *Xenopus* oocytes 3 days after injection of 4 ng of wild-type TRPV4 cRNA presented small currents that could be greatly amplified by the addition of the synthetic phorbol ester activator 4α-PDD at 3 μM (n > 30) (Fig. 1*a*, *upper*) (23). As expected of TRPV4, these currents show prominent outward rectification (24). Uninjected oocytes (n > 10) or those injected with TRPV4 cRNA with a M680K mutation engineered at the presumed filter (15) showed no such currents (n > 10) (Fig. 1*a*, *lower*). Perfusion of a hypotonic solution also activated these currents over minutes, which subsided upon return to isotonicity (n > 10). This cycle could be repeated with the same oocyte except when blocked by the TRP blocker ruthenium red (Fig. 1*b*). Although a native stretch activated channel is observed in excised patches from oocytes, hypotonicity fails to activate currents in the majority of whole oocytes examined by two-electrode voltage clamp (25).

Oocytes injected with 4 ng of cRNA of the brachyolmia-causing R616Q mutant allele presented very large currents even without 4α-PDD or hypotonicity, the magnitudes of which are greater compared with oocytes injected with 10-fold more wild-type cRNA (Fig. 1*c*). Despite variations, expressed currents clearly increased with the amount of cRNA injected. Assuming the same production of channels per unit injected RNA, comparisons show that the R616Q channel had ∼30 times the steady-state activities of the wild-type channel (Fig. 1*d*). R616Q-expressing oocytes exhibited macroscopic currents that showed outward rectification, ruthenium red blockage, and stimulation by 4α-PDD and hypotonicity like the wild type (data not shown). Oocytes rarely survived injection of >40 ng of wild-type TRPV4 cRNA or >4 ng of R616Q cRNA. The toxicity of stronger TRPV4 GOF mutants selected through yeast genetics has also been observed (23).

Unitary Conductance—Inside-out patches excised from TRPV4-expressing oocytes exhibited a large unitary conduct-
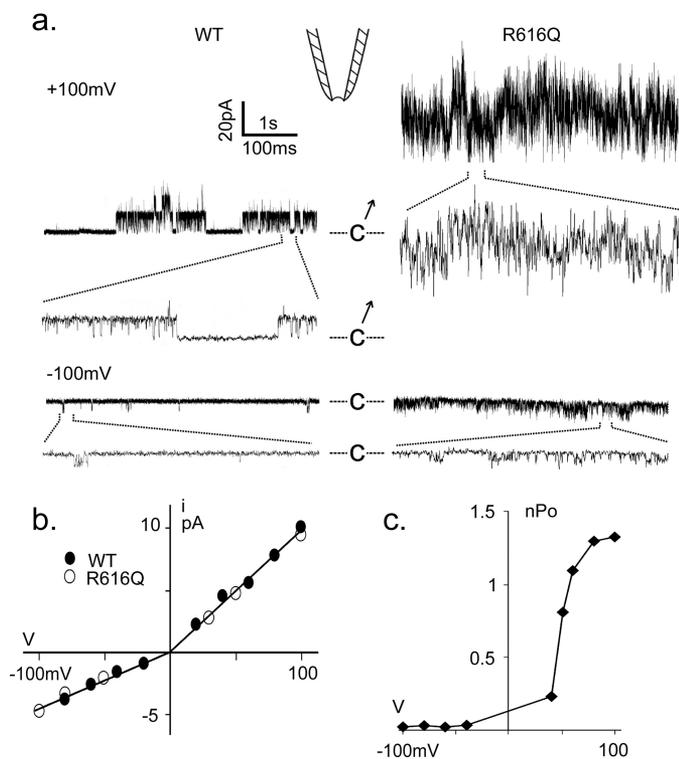
FIGURE 2. **Spontaneous microscopic TRPV4 currents.** *a*, spontaneous single-channel activities from a patch excised from an oocyte highly expressing the wild type (*left*) and a typical one expressing R616Q (*right*) examined at +100 mV (*upper*) or −100 mV (*lower*). Segments of the recordings are displayed at a faster time base showing discrete opening and closing events. *C* marks the closed levels. *b*, *I-V* plots showing the unitary conductances of the wild type (●) and R616Q (○). *c*, nP_o-*V* plot from a typical wild-type TRPV4-expressing patch showing activation by positive voltages.

ance, not observed in uninjected oocytes or those injected with filter mutant M680K RNA (data not shown). The spontaneous activities of wild-type or R616Q channels tended to run down immediately after patch excision. Channel activity was allowed to relax to a more stable level before quantification (Fig. 2a). *I-V* plots of both the wild-type and R616Q channels show unitary conductance rectification, being 98 picosiemens outward and 45 picosiemens inward (Fig. 2b), easily distinguishable from the ~30-picosiemen conductance native to the oocyte (supplemental Fig. S1) (26), which sometimes appeared in the same patches. The activity of TRPV4 could also be distinguished from that of this native channel by its 4α-PDD activation and time-dependent blockage by ruthenium red back-filled in the patch pipette (data not shown). Ensemble open probabilities (nP_o) of wild-type and mutant channels were small at negative voltages and increased steeply at positive voltages (Fig. 2, *a* and *c*). Matching the amount of cRNA injected and incubation period, the R616Q patches invariably had higher basal activities than the wild-type patches. Activation of multiple R616Q channels at positive voltage gave a noisy impression (Fig. 2a); however, the unitary conductance of R616Q could nonetheless be measured from the basal activities of oocytes injected with less RNA (see Fig. 5) or at negative potential (Fig. 2a).

Suction Activates TRPV4—Tens of mm Hg suction pulses applied to membrane patches excised from expressing oocytes directly activated TRPV4 channels (from >200 patches of >50

oocytes). Such activations are shown in the sample traces in Fig. 3a for the wild-type channel and in Fig. 5 (*a*, *b*, *f*, and *g*) for the R616Q mutant channel. From the same excised patches, after the rundown of spontaneous activities, nP_o increased with the pipette suction (Fig. 3, *b* and *c*). This increased nP_o was maintained over the course of 10−20 s of pressure exposure (*e.g.* Fig. 5, *a*, *b*, *f*, and *g*), and in the cases in which pressure sensitivities were assessed before patch excision, no significant changes were observed after excisions (data not shown). In no instances could the TRPV4 nP_o reach saturation before the applied suction ruptured the patch or the seal at ~60−200 mm Hg. Starting with sizable spontaneous activities, the nP_o of R616Q TRPV4 increased 3−4-fold, with a 10−15% S.E. between 0- and 60-mm Hg suction (Fig. 3c, *open symbols*; and Fig. 5, *b* and *j*). A similar rise in the wild-type nP_o was seen between 30- and 60-mm Hg suction (Fig. 3c, *closed symbols*). The R616Q basal activities appeared to cause a left shift of the nP_o *versus* force response curve, but variability and other technical limitations precluded slope comparison (Fig. 3c). The basal activities of the wild type among different patches were low and variable. Estimation of mechanosensitivity as the -fold increase in nP_o by suction was therefore carried out with R616Q instead of the wild type.

A PLA2 Inhibitor Blocks General Activation of TRPV4 in Intact Oocytes—It has been reported that hypotonic but not 4α-PDD activation of TRPV4 expressed in cultured cells can be blocked by preincubating them for 20 min in the presence of the PLA2 inhibitor bromophenacyl bromide (BPB) at 100 μM (3). Similar treatment had no effect on the ability of hypotonicity or 4α-PDD to activate TRPV4 in whole oocytes. Because of the possibility that the access of BPB was restricted by the large size and complex geometry of the oocyte, we extended the incubation time for several hours. Indeed, we found that the hypotonic response was greatly inhibited by extended incubation (Fig. 4, *a* and *c*). However, we found that the 4α-PDD response was also reduced (Fig. 4, *b* and *d*) in fact to a greater extent (Fig. 4e). It thus appears that BPB can greatly inhibit the ability of either 4α-PDD or hypotonicity (but not depolarization) to activate TRPV4 in intact oocytes. In previous work, the apparent specificity of BPB inhibition of the hypotonic response could have reflected a partial inhibition of PLA2 due to the shorter incubation, resulting in obvious inhibition of only the weaker hypotonic response. It is notable that depolarization activation was not substantially affected by BPB in the absence of additional stimulation, underscoring the independence of voltage- from chemical- and mechanical-dependent gating (23). Anthranilic acid, another PLA2 inhibitor, at 20 μM for 15 min (27) also had no effect on the TRPV4 hypotonic response. 1 h of treatment with 50 μM anthranilic acid was toxic to oocytes.

Blockers of 5′,6′-Epoxyeicosatrienoic Acid Synthesis Have No Effect on the Direct Mechanosensitivity of TRPV4 in Excised Patches—We quantified the effects of PLA2 or EPG inhibitors on the mechanosensitivities of R616Q and wild-type alleles of oocyte-expressed TRPV4 in excised patches as well. Ten R616Q membrane patches were sampled, and their responses to 60-mm Hg pipette suctions were registered as controls. This procedure was repeated on oocytes preincubated in BPB (Fig. 5, *upper panels*) or 17-octadecynoic acid, an inhibitor of EPG (3,
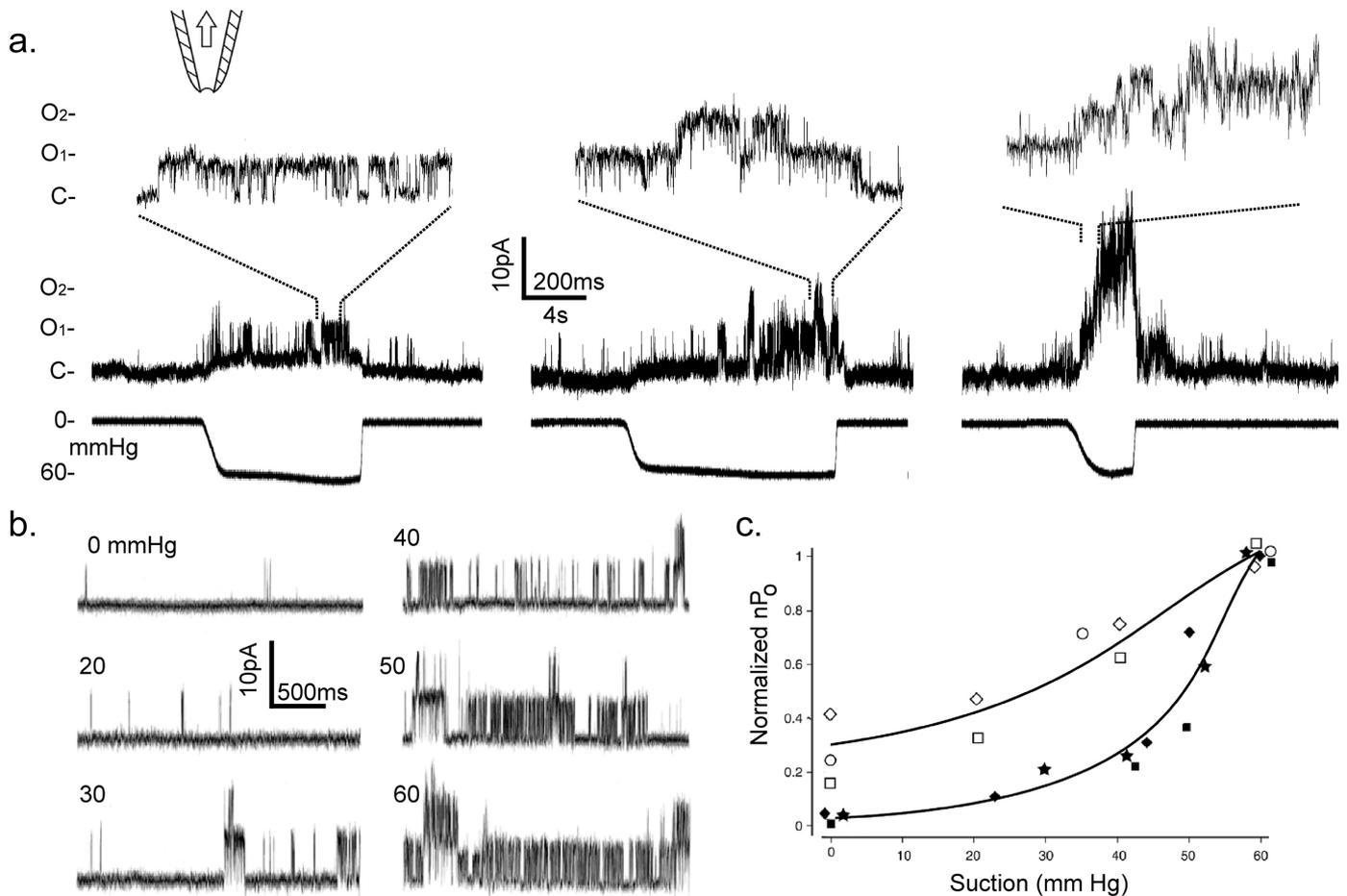
FIGURE 3. **Direct activation of wild-type TRPV4 by membrane stretch.** *a*, sample of raw traces of average quality from three patches excised from three different oocytes, showing activation by 60-mm Hg suctions applied to excised patches held at $+50$ mV under a patch clamp. The *upper traces* are displayed at a faster time base to show unitary transitions between closed (*C*) and open (*O1* and *O2*) levels. *b*, sample traces from a high-quality wild-type patch subjected to a range of pipette suctions recorded with a pipette solution of 98 mM KCl, 1 mM $MgCl_2$, and 20 mM Na^+ citrate, pH 4.5. *c*, plot of nP_o *versus* suction of the wild type (*filled symbols*) and R616Q (*open symbols*). nP_o values from three patches each are normalized to that at 60 mm Hg. Different symbols are different typical patches chosen to show the trend as well as variability; *curves* are segments of symmetric sigmoidal fits overlayed by eye.
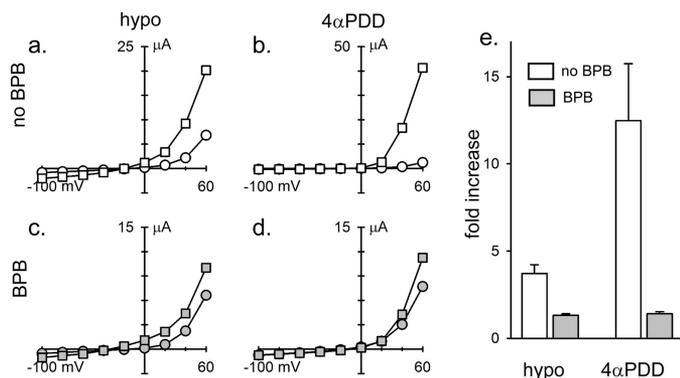
FIGURE 4. **BPB inhibits both the hypotonic and 4α-PDD responses in intact oocytes.** Unexposed oocytes (*a* and *b*) or those incubated for 5–9 h in 100 μM BPB (*c* and *d*) were subjected to 1-s voltage steps of between -100 and 60 mV either before (*circles*) or after (*squares*) exposure to hypotonicity (*hypo*; as described in the legend to Fig. 1) for 10 min (*a* and *c*) or to 3 μM 4α-PDD for 20 min (*b* and *d*). BPB was present during experimentation as well in *c* and *d*. Plotted are peak currents *versus* test potentials. *e* shows the relative increase in the peak response at 60 mV in the absence (*white bars*) or presence (as in *c* and *d*; *gray bars*) of BPB to hypotonicity (*left*) or 4α-PDD (*right*) (mean ± S.E., n = 4). Note that the apparent smaller response to hypotonicity in *e* compared with that shown in Fig. 1*b* reflects that it was assessed at 60 mV here as opposed to 20 mV in Fig. 1*b*, and hypotonicity appears to cause a slight leftward shift in the *G-V* relationship, as can be seen in *a*.

16) (Fig. 5, *lower panels*) for 1–3 h. The inhibitors were also present in the recording chamber, where they had direct access to the excised membrane patches. No significant changes in channel responses to suctions were observed upon incubation of these inhibitors. Qualitatively similar results were also obtained with the wild-type channels, with no difference in the mechanosensitivity observed after inhibitor exposure (data not shown). Thus, the direct mechanosensitivity of TRPV4 in excised patches seems to be independent of the production of arachidonic acid or its metabolite 5′,6′-epoxyeicosatrienoic acid.

DISCUSSION

We found rat TRPV4 to respond directly to pipette suctions that stretch the excised membrane patches. This mechanosensitivity was robust and consistent, observed in >200 wild-type or R616Q mutant patches (Figs. 3 and 5). The response of TRPV4 to stretch force in excised patches bathed in a simple buffer rules out any covalent chemistry dependent on diffusible cytoplasmic factors being involved in transduction.

Inhibition of either PLA_2 by BPB or EPG by 17-octadecynoic acid had no effect on the direct mechanosensitivity of TRPV4 in excised patches (Fig. 5). However, prolonged exposure to BPB
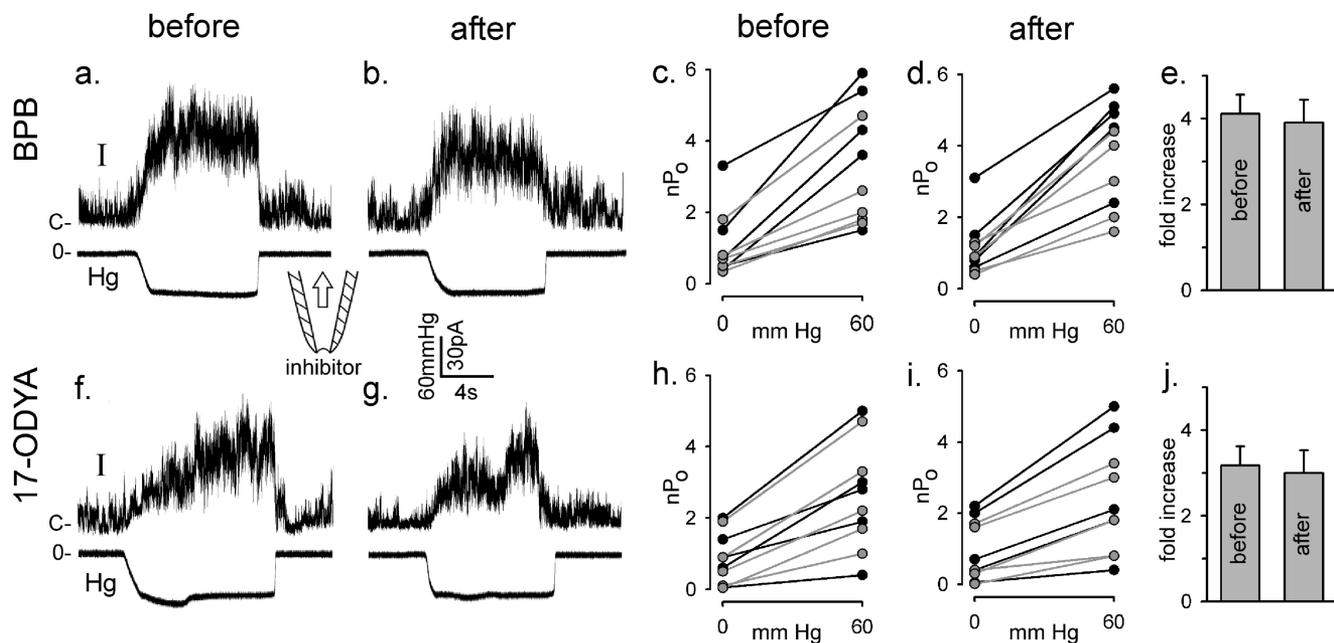
FIGURE 5. **Enzyme inhibitors do not alter TRPV4 mechanosensitivity in excised patches.** Five patches were excised from each of two R616Q-expressing oocytes held at +50 mV before and another 5 × 2 patches excised after 30 min of incubation in the presence of 200 μM BPB (*upper panels*). *a* and *b* show sample traces of the response to suctions. *c* shows nP_o increases by 60-mm Hg suctions in five different patches from one oocyte (*black lines*) and five from a second oocyte (*gray lines*) before the BPB treatment. *d* shows nP_o increases by the same suctions of five new patches from the first oocyte (*black lines*) and five others from the second oocyte (*gray lines*) sampled after the BPB treatment. *e* summarizes the -fold increase in nP_o from 0- to 60-mm Hg suction. (Those with $nP_o \sim 0$ without suction are excluded in the calculation.) *f–j* show parallel experimental results with 100 μM 17-octadecynoic acid (*17-ODYA*).

strongly inhibited both the hypotonic and 4α-PDD responses of intact oocytes (Fig. 4). This could reflect a Ca^{2+}-dependent feedback mechanism that could facilitate an all-or-none response of TRPV4 to stimulation. PLA_2 requires Ca^{2+} binding to its C2 domain for activity (28). Threshold initial Ca^{2+} entry through the force-gated TRPV4 could subsequently activate the Ca^{2+}-PLA_2-EPG-5′,6′-epoxyeicosatrienoic acid pathway to provide a positive feedback to enhance the TRPV4 Ca^{2+} influx. BPB would block such a feedback. Such a Ca^{2+}-induced Ca^{2+} release feedback is fairly common and has been documented for the mechanosensitive TRPY1 (11, 13).

Beyond the control of systemic osmolarity (1, 29), TRPV4 has been implicated in other force-related transductions *in vivo*, including flow-mediated dilation of arteries (30), strain-induced endothelial cell reorientation (31), viscosity-coupled epithelial ciliary activity (32, 33), and osteoclast response to weight load on bones (19). In these instances, a direct mechanosensitivity of the TRPV4 channel itself provides the simplest explanation.

We encountered patch-to-patch heterogeneity, which may reflect differences in patch elasticity or other geometric and mechanical complexities of the membrane (34) with its subtending cytoskeleton (35, 36) and/or heterogeneity of the channel populations (*e.g.* degree of phosphorylation?). These intricacies are beyond the ability of the present technical resolution to sort out and may underlie the statistical variances reported within studies (3, 16) and contradictory claims between studies (1, 2, 14) found in the TRPV4 literature.

Recent discoveries on heritable human diseases due to TRPV4 mutations illustrate the medical importance of TRPV4 (4, 27). We found the brachyolmia-causing R616Q allele to retain wild-type unitary conductance and rectification but to have constitutive activities in the absence of applied stimuli

(Figs. 1–4). R616 is predicted to be at the base of the fifth transmembrane helix (S5) in the TRPV4 subunit. Recent forward genetic screening for TRPV4 mutations that are toxic to yeast yielded GOF alleles nearby (L619P, L624P). These yeast-selected mutations have similar but much stronger GOF phenotypes than R616Q (23). These findings support a general *Shaker*-like topology for TRPV4, with S5 being part of the main gate. Because the mutant channel has direct mechanosensitivity and constitutive activities, it likely behaves in osteoclasts or other relevant cells as a wild-type channel under mechanical stress, leading to the GOF phenotypes *in vivo* (4, 5). High-resolution analyses of other disease-causing alleles under patch clamps should further our understanding of the disease process.

REFERENCES

1. Liedtke, W., Choe, Y., Martí-Renom, M. A., Bell, A. M., Denis, C. S., Sali, A., Hudspeth, A. J., Friedman, J. M., and Heller, S. (2000) *Cell* **103,** 525–535
2. Strotmann, R., Harteneck, C., Nunnenmacher, K., Schultz, G., and Plant, T. D. (2000) *Nat. Cell Biol.* **2,** 695–702
3. Vriens, J., Watanabe, H., Janssens, A., Droogmans, G., Voets, T., and Nilius, B. (2004) *Proc. Natl. Acad. Sci. U.S.A.* **101,** 396–401
4. Rock, M. J., Prenen, J., Funari, V. A., Funari, T. L., Merriman, B., Nelson, S. F., Lachman, R. S., Wilcox, W. R., Reyno, S., Quadrelli, R., Vaglio, A., Owsianik, G., Janssens, A., Voets, T., Ikegawa, S., Nagai, T., Rimoin, D. L., Nilius, B., and Cohn, D. H. (2008) *Nat. Genet.* **40,** 999–1003
5. Camacho, N., Krakow, D., Johnykutty, S., Katzman, P. J., Pepkowitz, S., Vriens, J., Nilius, B., Boyce, B. F., and Cohn, D. H. (2010) *Am. J. Med.*

Genetics **152A,** 1169–1177

6. Kung, C. (2005) *Nature* **436,** 647–654
7. Christensen, A. P., and Corey, D. P. (2007) *Nat. Rev. Neurosci.* **8,** 510–521
8. Lumpkin, E. A., and Caterina, M. J. (2007) *Nature* **445,** 858–865
9. Patel, A. J., Lazdunski, M., and Honoré, E. (2001) *Curr. Opin. Cell Biol.* **13,** 422–428
10. Lesage, F., and Lazdunski, M. (2000) *Am. J. Physiol. Renal Physiol.* **279,** F793–F801
11. Su, Z., Zhou, X., Loukin, S. H., Haynes, W. J., Saimi, Y., and Kung, C. (2009) *Pflugers Arch.* **458,** 861–867
12. Nilius, B., Watanabe, H., and Vriens, J. (2003) *Pflugers Arch.* **446,** 298–303
13. Zhou, X. L., Batiza, A. F., Loukin, S. H., Palmer, C. P., Kung, C., and Saimi, Y. (2003) *Proc. Natl. Acad. Sci. U.S.A.* **100,** 7105–7110
14. Suzuki, M., Mizuno, A., Kodaira, K., and Imai, M. (2003) *J. Biol. Chem.* **278,** 22664–22668
15. Liedtke, W., Tobin, D. M., Bargmann, C. I., and Friedman, J. M. (2003) *Proc. Natl. Acad. Sci. U.S.A.* **100,** Suppl. 2, 14531–14536
16. Watanabe, H., Vriens, J., Prenen, J., Droogmans, G., Voets, T., and Nilius, B. (2003) *Nature* **424,** 434–438
17. Loukin, S. H., Su, Z., and Kung, C. (2009) *FEBS Lett.* **583,** 754–758
18. Köttgen, M., Buchholz, B., Garcia-Gonzalez, M. A., Kotsis, F., Fu, X., Doerken, M., Boehlke, C., Steffl, D., Tauber, R., Wegierski, T., Nitschke, R., Suzuki, M., Kramer-Zucker, A., Germino, G. G., Watnick, T., Prenen, J., Nilius, B., Kuehn, E. W., and Walz, G. (2008) *J. Cell Biol.* **182,** 437–447
19. Mizoguchi, F., Mizuno, A., Hayata, T., Nakashima, K., Heller, S., Ushida, T., Sokabe, M., Miyasaka, N., Suzuki, M., Ezura, Y., and Noda, M. (2008) *J. Cell Physiol.* **216,** 47–53
20. Krakow, D., Vriens, J., Camacho, N., Luong, P., Deixler, H., Funari, T. L., Bacino, C. A., Irons, M. B., Holm, I. A., Sadler, L., Okenfuss, E. B., Janssens, A., Voets, T., Rimoin, D. L., Lachman, R. S., Nilius, B., and Cohn, D. H. (2009) *Am. J. Hum. Genet.* **84,** 307–315
21. Loukin, S. H., Vaillant, B., Zhou, X. L., Spalding, E. P., Kung, C., and Saimi, Y. (1997) *EMBO J.* **16,** 4817–4825
22. Goldin, A. L. (1992) *Methods Enzymol.* **207,** 266–279
23. Loukin, S., Su, Z., Zhou, X., and Kung, C. (2010) *J. Biol. Chem.* **285,** 19884–19890
24. Everaerts, W., Nilius, B., and Owsianik, G. (2009) *Prog. Biophys. Mol. Biol.*, in press
25. Zhang, Y., and Hamill, O. P. (2000) *J. Physiol.* **523,** 83–99
26. Maroto, R., Raso, A., Wood, T. G., Kurosky, A., Martinac, B., and Hamill, O. P. (2005) *Nat. Cell Biol.* **7,** 179–185
27. Nilius, B., and Owsianik, G. (2010) *Nat. Genet.* **42,** 98–100
28. Burke, J. E., and Dennis, E. A. (2009) *J. Lipid Res.* **50,** (suppl.) S237–S242
29. Liedtke, W. (2008) *Ann. N.Y. Acad. Sci.* **1144,** 42–52
30. Mendoza, S. A., Fang, J., Gutterman, D. D., Wilcox, D. A., Bubolz, A. H., Li, R., Suzuki, M., and Zhang, D. X. (2010) *Am. J. Physiol. Heart Circ. Physiol.* **298,** H466–H476
31. Thodeti, C. K., Matthews, B., Ravi, A., Mammoto, A., Ghosh, K., Bracha, A. L., and Ingber, D. E. (2009) *Circ. Res.* **104,** 1123–1130
32. Andrade, Y. N., Fernandes, J., Vázquez, E., Fernández-Fernández, J. M., Arniges, M., Sánchez, T. M., Villalón, M., and Valverde, M. A. (2005) *J. Cell Biol.* **168,** 869–874
33. Lorenzo, I. M., Liedtke, W., Sanderson, M. J., and Valverde, M. A. (2008) *Proc. Natl. Acad. Sci. U.S.A.* **105,** 12611–12616
34. Suchyna, T. M., Markin, V. S., and Sachs, F. (2009) *Biophys. J.* **97,** 738–747
35. Zhang, Y., and Hamill, O. P. (2000) *J. Physiol.* **523,** 101–115
36. Zhang, Y., Gao, F., Popov, V. L., Wen, J. W., and Hamill, O. P. (2000) *J. Physiol.* **523,** 117–130